

Nanomeasurements of individual carbon nanotubes by *in situ* TEM*

Z. L. Wang^{1†}, P. Poncharal², and W. A. de Heer^{2†}

¹School of Materials Science and Engineering, ²School of Physics, Georgia Institute of Technology, Atlanta, Georgia 30332 USA

Abstract: Property characterization of nanomaterials is challenged by the small size of the structure because of the difficulties in manipulation. Here we demonstrate a novel approach that allows a direct measurement of the mechanical and electrical properties of individual nanotube-like structures by *in situ* transmission electron microscopy (TEM). The technique is powerful in a way that it can be directly correlated to the atomic-scale microstructure of the carbon nanotube with its physical properties, thus providing a complete characterization of the nanotube. Applications of the technique will be demonstrated in measurements of the mechanical properties, the electron field emission, and the ballistic quantum conductance of individual carbon nanotubes. A nanobalance technique is demonstrated that can be applied to measure the mass of a single tiny particle as light as 22 fg ($1 \text{ f} = 10^{-15}$).

INTRODUCTION

Nanoscience and nanotechnology, as a main research thrust in the 21st century, depend on materials preparation, property characterization, device fabrication, and system integration. Due to the high size- and structure-selectivity of nanomaterials, their physical properties could be quite diverse, depending on their atomic-scale structure, size, and chemistry [1]. To maintain and utilize the basic and technological advantages offered by the size-specificity and -selectivity of the nanomaterials, it is essential to develop new techniques that can quantitatively measure the properties of individual nanomaterials, such as a single nanoparticle or a carbon nanotube, with well-defined structures.

Characterizing the properties of individual nanostructures is a challenge to many existing testing and measuring techniques because of the following constraints. First, the size (diameter and length) is rather small, prohibiting the applications of well-established testing techniques. Tensile and creep testing of a fiber-like material, for example, require that the size of the sample be sufficiently large to be clamped rigidly by the sample holder without sliding. This is impossible for nanostructured fibers using conventional means. Secondly, the small size of the nanostructures makes their manipulation rather difficult, and specialized techniques are needed for picking up and installing individual nanostructures. Therefore, new methods and methodologies must be developed to quantify the properties of individual nanostructures.

Among the various techniques, scanning probe microscopy (STM, AFM) has been a major tool in investigating the properties of individual nanostructures. This is a powerful approach in probing the properties of nanostructures. We have recently developed a novel approach which uses *in situ* transmission electron microscopy (TEM) [2,3] as an effective tool for measuring the properties of individual carbon nanotubes. This is a new technique that not only can provide the properties of an individual nanotube, but also can give the structure of the nanotube through electron imaging and diffraction,

*Pure Appl. Chem. 72, 1–331 (2000). An issue of reviews and research papers based on lectures presented at the 1st IUPAC Workshop on Advanced Materials (WAM1), Hong Kong, July 1999, on the theme of nanostructured systems.

†Corresponding authors: zhong.wang@mse.gatech.edu; dheer@electra.physics.gatech.edu

providing an ideal technique for understanding the property–structure relationship. The objective of this paper is to review our recent progress in applying *in situ* TEM for characterizing the electrical, mechanical, and field-emission properties of carbon nanotubes, aiming at pointing out a new direction in nanomeasurements.

EXPERIMENTAL METHOD

TEM is a powerful tool for characterizing the atomic-scale structures of solid-state materials. A modern TEM is a versatile machine that not only can provide a real-space resolution better than 0.2 nm, but also can give a quantitative chemical and electronic analysis from a region as small as 1 nm. It is feasible to receive a full structure characterization from TEM. A powerful and unique approach could be developed if we could integrate the structural information of a nanostructure provided by TEM with the properties measured from the same nanostructure by *in situ* TEM. Thus, a one-to-one correspondence can be achieved, providing a model system for comprehensively understanding nanomaterials.

To carry out the property measurement of a nanotube, a specimen holder for a JEOL 100C TEM (100 kV) was built for applying a voltage across a nanotube and its counter electrode (Fig. 1) [4]. The specimen holder requires the translation of the nanotube via either mechanical movement by a micrometer or axial directional piezo. The static and dynamic properties of the nanotubes can be obtained by applying a controllable static and alternating electric field. The nanotubes were produced by an arc-discharge technique, and the as-prepared nanotubes were agglomerated into a fiber-like rod. The carbon nanotubes have diameters of 5–50 nm and lengths of 1–20 μm , and most of them are nearly defect-free. The fiber was glued using silver paste onto a gold wire, through which the electric contact was made. The counter electrode can be a droplet of mercury or galium for electric contact measurement or an Au/Pt ball for electron field-emission characterization.

The nanotube to be used for property measurement is directly imaged under TEM (Fig. 2), and electron diffraction patterns and images can be recorded from the nanotube. The information provided by TEM directly reveals both the surface and the intrinsic structure of the nanotube. This is a unique advantage over the SPM techniques. The distance from the nanotube to the counter electrode is control-

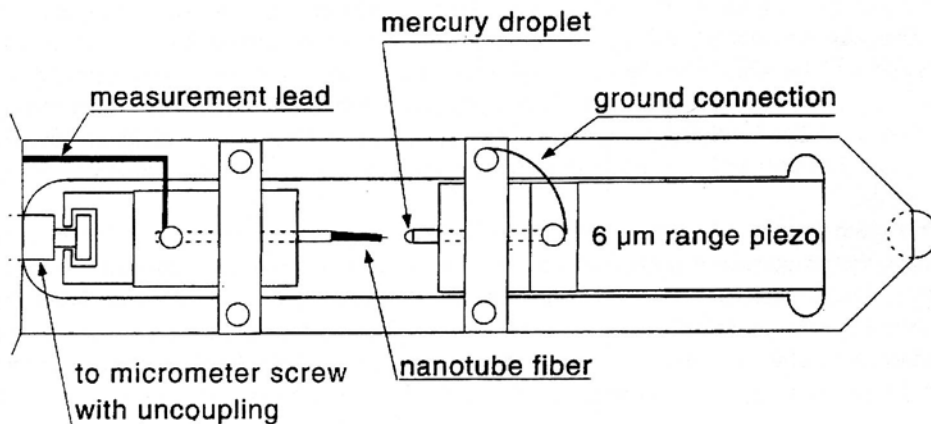


Fig. 1 Schematic diagram of the specimen holder for *in situ* measurement in TEM.

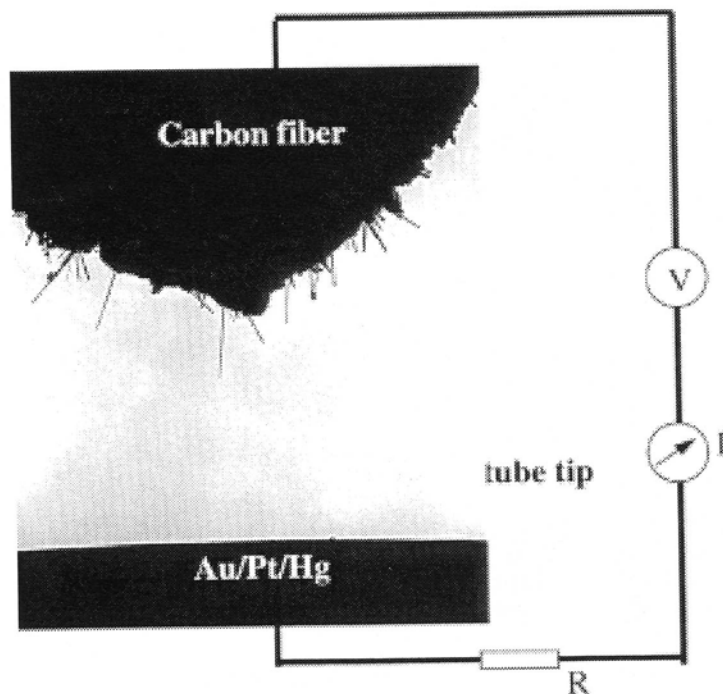


Fig. 2 TEM image showing carbon nanotubes at the end of the electrode and the other counter electrode. A constant or alternating voltage can be applied to the two electrodes to induce electrostatic deflection or mechanical resonance.

lable. An electric potential is applied across the electrodes to carry out a variety of measurements, to be described in following sections.

EXPERIMENTAL RESULTS

One of the significant challenges in nanoscience is the measurement of mechanical properties of individual constituents that comprise the nanosystem. The problem arises due to difficulties in gripping and handling fibers that have nano-size diameters. Mechanical characterization of individual nanofibers has relied on AFM. By deflecting on one end of the nanofiber with an AFM tip and holding the other end fixed, the mechanical strength has been calculated by correlating the lateral displacement of the fiber as a function of the applied force [5,6]. This type of measurement has two major limitations. The deformation of the tip was not considered in the calculation, and the tip–fiber contact and interface sliding were ignored.

Previously, mechanical properties of a carbon nanotube have been measured by *in situ* TEM based on the thermal vibration amplitude of a carbon nanotube [7]. Figure 3 shows a TEM image recorded from carbon nanotubes grown by arc-discharge. A few nanotubes are indicated by arrowheads, which show blurring contrast toward the ends as a result of thermal vibration. But a quantitative measurement of the vibration amplitude could be rather inaccurate, thus, the calculated bending modulus showed a large error. This technique is likely to be appropriate for nanotubes with smaller diameters and longer lengths because the ones with larger diameters show no visible thermal vibration.

Electrostatic bending of a single carbon nanotube

Our approach is based on the electric-field-induced static and dynamic phenomena [2]. The carbon nanotube can be charged by an externally applied voltage. The induced charge is distributed mostly at the tip of the carbon nanotube, and the electrostatic force results in the deflection of the nanotube. Figure 4 shows a series of TEM images for two nanotubes attached to the two electrodes under different

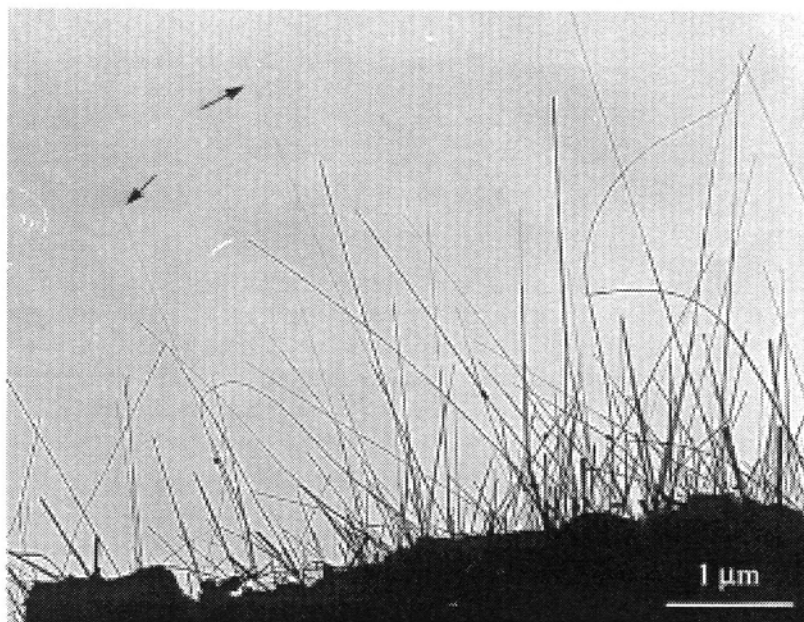


Fig. 3 A typical TEM image showing the multi-walled carbon nanotubes produced by arc-discharge, that were used for the measurements presented in this paper.

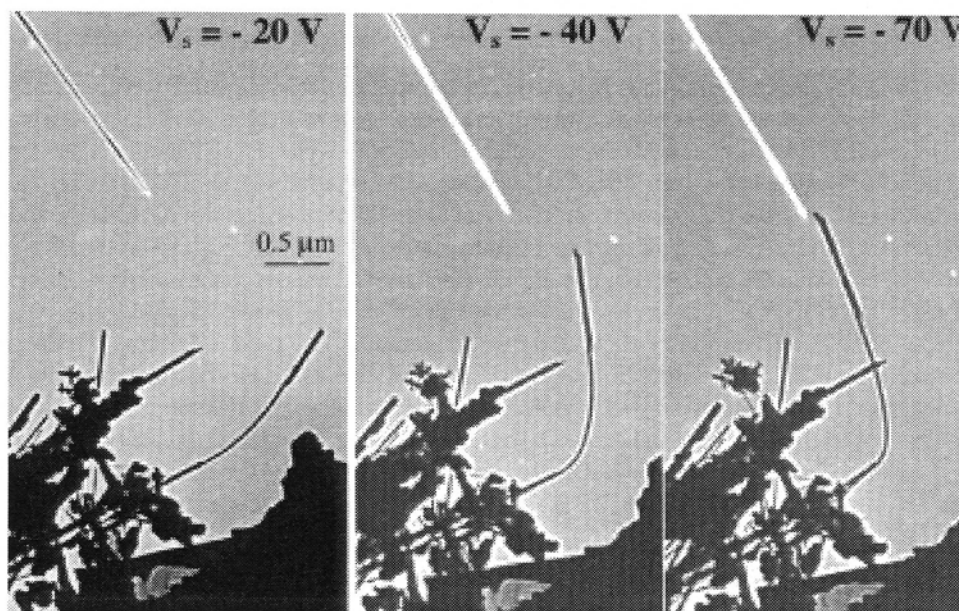


Fig. 4 Electrostatic attraction between two carbon nanotubes induced by a constant field across the electrodes. The induced charges are mainly accumulated at the tip.

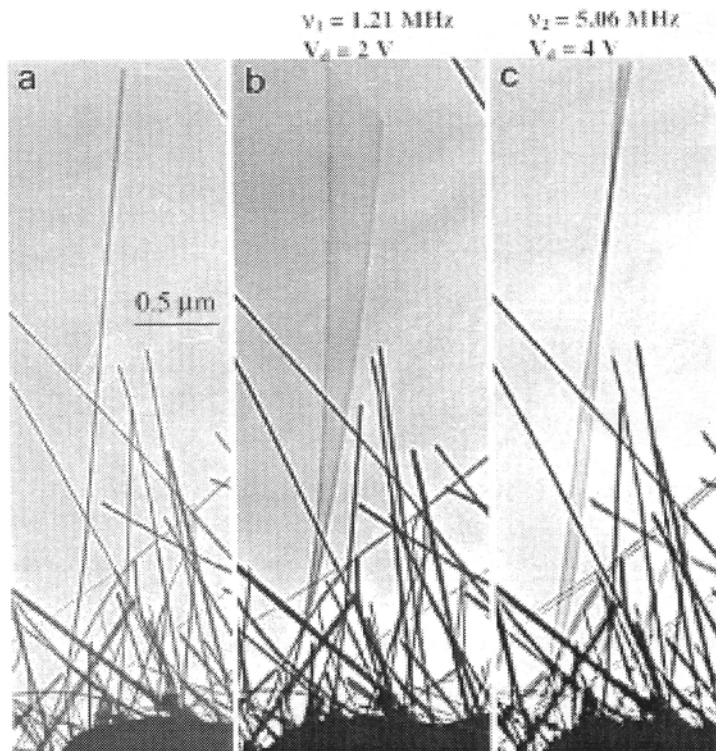


Fig. 5 A selected carbon nanotube at (a) stationary, (b) the first harmonic resonance ($\nu_1 = 1.21$ MHz) and (c) the second harmonic resonance ($\nu_2 = 5.06$ MHz).

applied voltages. The tips of the nanotubes attract with each other, and the bright and dark contrast of the two tubes is due to the opposite charges built on the tubes. The nanotube is a very flexible structure, and it can be bent for more than 90° , after which it recovers its original shape.

Bending modulus of a carbon nanotube

To measure the bending modulus of a carbon nanotube, an oscillating voltage is applied to the nanotube, with the ability to tune the frequency of the applied voltage. Resonance can be induced in carbon nanotubes by tuning the frequency (Fig. 5). Resonance is nanotube-selective because the natural vibration frequency depends on the tube outer diameter (D), inner diameter (D_1), the length (L), the density (ρ), and the bending modulus (E_b) of the nanotube [8]:

$$\nu_i = \frac{\beta_i^2}{8\pi} \frac{1}{L^2} \sqrt{\frac{(D^2 + D_1^2)E_b}{\rho}} \quad (1)$$

where $\beta_1 = 1.875$ and $\beta_2 = 4.694$ for the first and the second harmonics.

The correlation between the applied frequency and the resonance frequency of the nanotube is not trivial. From the data shown in the section "Electrostatic bending of a single carbon nanotube", we know that there are some electrostatic charges built on the tip of the carbon nanotube. With consideration of the difference between the surface work functions between the carbon nanotube and the counter electrode (Hg or Au), a static charge exists even when the applied voltage is withdrawn. Therefore, under an applied field the induced charge on the carbon nanotube can be represented by $Q = Q_0 + \alpha V_0 \cos \omega t$, where Q_0 represents the charge on the tip to balance the difference in surface work

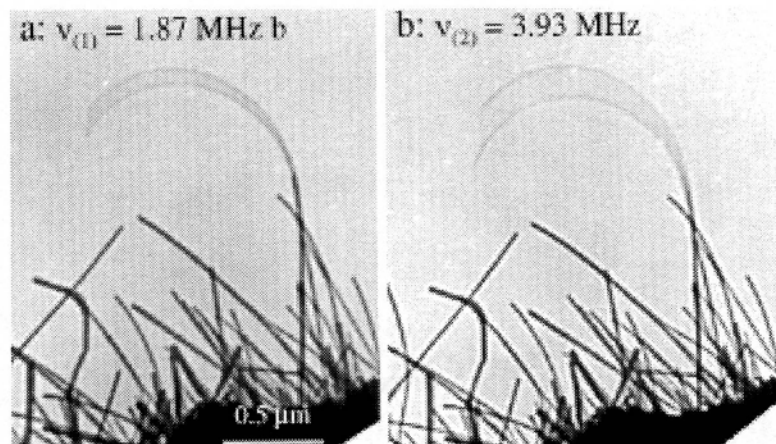


Fig. 6 Resonance of a bent carbon nanotube at (a) $v_{(1)} = 1.87$ MHz, $V_0 = 2$ V and (b) $v_{(2)} = 3.93$ MHz, $V_0 = 5$ V, showing the multiple harmonic effect.

functions, α is a geometrical factor, and V_0 is the amplitude of the applied voltage. The force acting on the carbon nanotube is

$$F = \beta(Q_0 + \alpha V_0 \cos\omega t) V_0 \cos\omega t = \alpha\beta V_0^2/2 + \alpha\beta V_0 \cos\omega t + \alpha\beta V_0^2/2 \cos 2\omega t, \quad (2)$$

where β is a proportional constant. Thus, resonance can be induced at ω and 2ω at vibration amplitudes proportional to V_0 and V_0^2 , respectively. The former is a linear term in which the resonance frequency equals the applied frequency, while the latter is a nonlinear term, and the resonance frequency is twice of the applied frequency. In practical experiments, the linear and nonlinear terms can be distinguished by observing the dependence of the vibration amplitude on the magnitude of the voltage V_0 .

Another factor that one needs to consider is to identify the true fundamental resonance frequency. From Eq. 1, the frequency ratio between the two modes $i = 1$ and $i = 2$ is 6.27. In practice, if resonance occurs at ω , resonance could also occur at 2ω , which is the second harmonic. Figure 6 shows the resonance of a bent nanotube in such a case. To identify the fundamental frequency, one needs to examine the resonance at a frequency that is half or close to half of the observed resonance frequency; if no resonance occurs, the observed frequency is the true fundamental frequency, then, Eq. 1 for $i = 1$ applies. Figure 6 also shows that our technique can be applied to determine the mechanical property of a deformed fiber-like material, which is an advantage over the SPM technique.

The diameters of the tube can be directly determined from TEM images at a high accuracy. The determination of length has to consider the 2D projection effect of the tube. It is essential to tilt the tube and to catch its maximum length in TEM, which is likely to be the true length. This requires a TEM that gives a tilting angle as large as of $\pm 60^\circ$. The vibration of the nanotube in Fig. 5b is not in the plane perpendicular to the beam. Also, the operation voltage of the TEM is important to minimize radiation damage. The 100-kV TEM used in our experiments showed almost no detectable damage to a carbon nanotube, while a 200-kV Hitachi HF-2000 TEM could quickly damage a nanotube within 10 min of beam illumination.

To trace the sensitivity of resonance frequency on beam illumination and radiation damage at 100 kV, a carbon nanotube was resonated for more than 30 min. The resonance frequency showed an increase of $\sim 1.4\%$ over the entire period of experiment (Fig. 7), but no dependence on the electron dose was found. The full width at half-maximum (fwhm) for the resonance peak was measured to be $\Delta v/v = 0.6\%$ in a vacuum of 10^{-4} to 10^{-5} torr. A slight increase in the resonance frequency could be

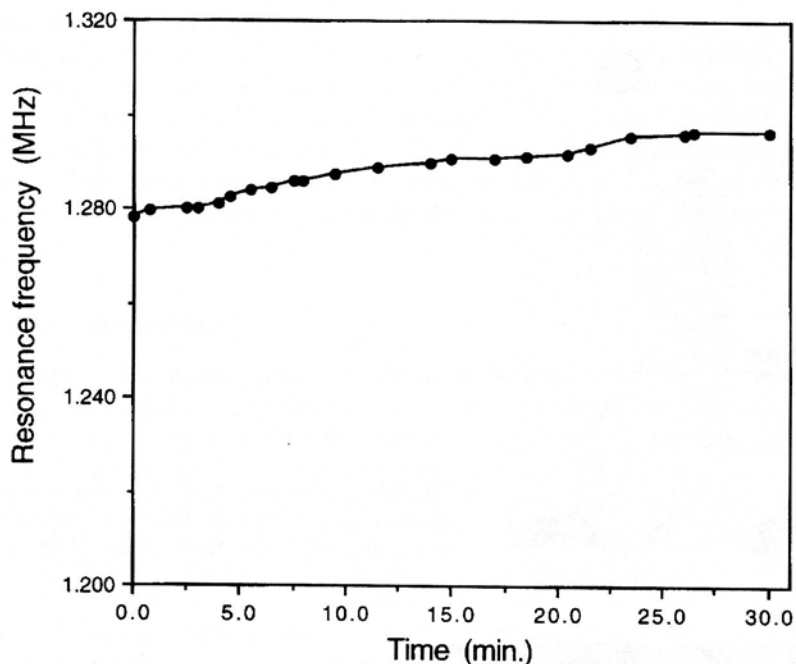


Fig. 7 Time dependence of the resonance frequency of a carbon nanotube, being illuminated by 100-kV electrons.

related to the change of carbon structure under the electron beam, but such a change has a negligible effect on the measurement of the bending modulus.

After a systematic study of the multi-walled carbon nanotubes, the bending modulus of nanotubes was measured as a function of their diameters [2]. The bending modulus is as high as 1.2 TPa (as strong as diamond) for nanotubes with diameters smaller than 8 nm, and it drops to as low as 0.2 TPa for those with diameters larger than 30 nm. A decrease in bending modulus as the increase of the tube diameter is attributed to the wrinkling effect of the wall of the nanotube during small bending. This effect almost vanishes when the diameters of the tubes are less than 12 nm.

Nanobalance of a single particle

In analogy to a spring pendulum, the mass of a particle attached at the end of the spring can be determined if the vibration frequency is measured, provided that the spring constant is calibrated. This principle can be adopted to the case outlined in the section "Bending modulus of a carbon nanotube" to determine a very tiny mass attached at the tip of the free end of the nanotube. The resonance frequency drops more than ~40% as a result of adding a small mass at its tip (Fig. 8). The mass of the particle can be thus derived by a simple calculation using an effective mass in the calculation of the momentum of inertia. This newly discovered "nanobalance" has been shown to be able to measure the mass of a particle as small as 22 ± 6 fg ($1\text{f} = 10^{-15}$). *This nanobalance is the most sensitive and smallest balance in the world.* We are currently applying this nanobalance to measure the mass of a single large biomolecule or a biomedical particle.

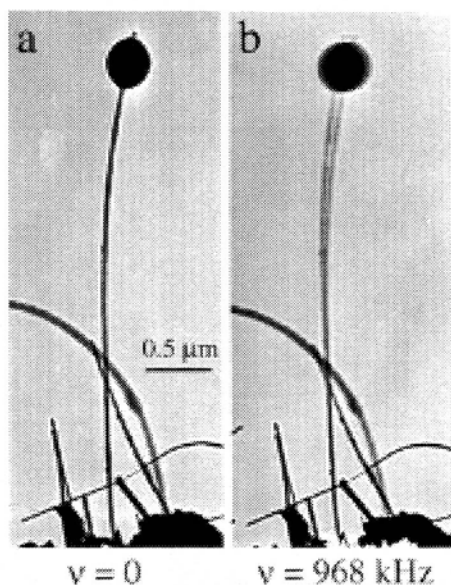


Fig. 8 A small particle attached at the end of a carbon nanotube at (a) stationary and (b) first harmonic resonance ($\nu = 0.968$ MHz). The effective mass of the particle measures ~ 22 fg ($1 \text{ f} = 10^{-15}$).

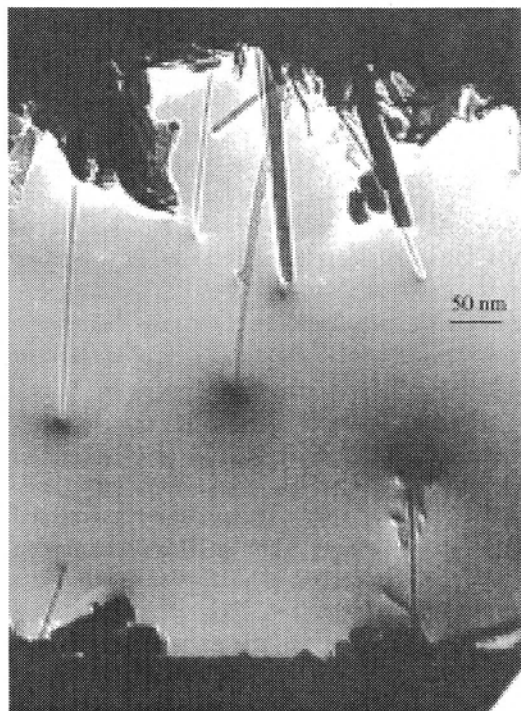


Fig. 9 *In situ* TEM observation of the electric-field-induced electron emission from carbon nanotubes. The applied voltage is 60 V, and the emission current ~ 20 μA .

Electron field emission from individual carbon nanotubes

The unique structure of carbon nanotubes clearly indicates that they are ideal objects that can be used for producing high field-emission current density in flat panel display [9]. Most of the current measurements were made using a film of the aligned carbon nanotubes, in which there is a large variation

in nanotube diameters and lengths, resulting in difficulty to clearly characterize the true switching-on field for electron field emission. Using the *in situ* TEM setup we built, the electric-field-induced electron emission of a single carbon nanotube has been studied. Figure 9 shows a TEM image of the carbon nanotubes that are emitting electrons at an applied voltage of 60 V. The dark contrast near the tips of the nanotube is the field contributed by the charges on the tip of the nanotube and the emitting electrons. A detailed analysis of the field distribution near the tip of the carbon nanotube by electron holography is being carried out, which is expected to provide the threshold field for field emission and many other properties.

Electric transport properties

Electrical properties of carbon nanotubes are rather attractive because of their importance in electronic devices. The conductance of a carbon nanotube has been measured using scanning tunneling microscopy [10] and four-point contact technique [11]. The results indicated a strong dependence of the conductance on the structure of the tube and its defects. We have measured the electric property of a single multi-walled carbon nanotube using the set-up of an atomic force microscope (AFM) [12]. A carbon fiber from the arc-discharge chamber was attached to the tip of the AFM, and the carbon tube at the forefront of the fiber was in contact with a liquid mercury bath. The conductance was measured as a function of the depth that the tube was inserted into the mercury. Surprisingly, the conductance shows quantized steps (Fig. 10), and the step height matches well to the quantum conductance $G_0 = 2e^2/h = 1/(12.9 \text{ k}\Omega)$. For a single tube, the conductance is G_0 , and the jump to $2G_0$ occurs once the second nanotube touches the mercury. Thus, the width of the step varies from experiment to experiment, but the step height is independent of the diameter or the length of the carbon nanotube, provided that the length is smaller than the electron mean-free path length. The quantum effect shows up only if the carbon nanotube is defect-free, which means the tubes produced by arc-discharge rather than catalytic growth. The flat plateaus of the conductance suggest that there is no residual resistance along the length of the nanotube. This is the result of ballistic conductance. This quantized effect for carbon nanotubes of diameters ~20–40 nm is believed to be the result of the conductance from the outermost single graphite layer.

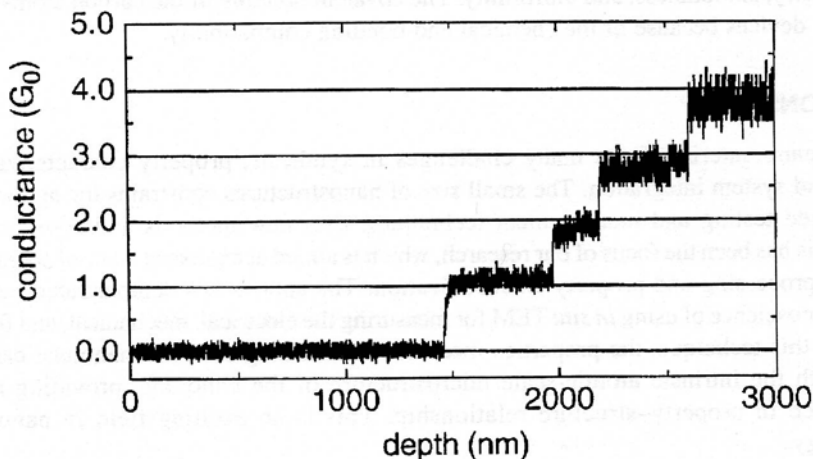


Fig. 10 Conductance of carbon nanotubes observed using the set-up in an AFM, showing the independence of the conductance of the depth into the liquid mercury in which the tip is being inserted. The second step is introduced as another nanotube touches the mercury.

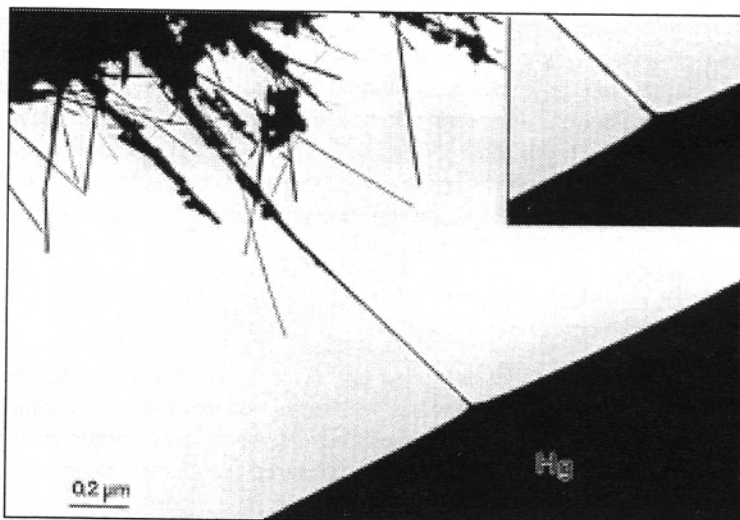


Fig. 11 *In situ* TEM image showing the contact of a carbon nanotube with a liquid mercury during the electric transport measurement.

Measurement using an alternative technique [13] confirmed our observation.

The experiment had been repeated in TEM using the *in situ* specimen holder illustrated in Fig. 1. Figure 11 shows the contact of a carbon nanotube with the mercury electrode. The conductance of G_0 was observed for a single nanotube. It is interesting to note that the contact area between the nanotube and the mercury surface is curved. This is likely due to the difference in surface work function between nanotube and mercury, which manifests itself as an electrostatic attraction and which distorts the mercury surface.

The observed quantum conductance may have great impact on molecular electronics. Carbon nanotubes could be used as interconnects for molecular devices without heat dissipation, with nicely defined geometry, smoothness, and uniformity. The covalent bonding of the carbon atoms is also a plus for molecular devices because of the chemical and bonding compatibility.

CONCLUSIONS

Research in nanomaterials faces many challenges in synthesis, property characterization, device fabrication, and system integration. The small size of nanostructures constrains the applications of the well-established testing and measurement techniques, thus new methods and approaches must be developed. This has been the focus of our research, which is aimed at exploring state-of-the-art techniques for materials processing and property characterization. The approaches demonstrated here are a new direction in nanoscience of using *in situ* TEM for measuring the electrical, mechanical, and field-emission properties. In this technique, the properties measured from a single carbon nanotube can be directly correlated with the intrinsic atomic-scale microstructure of the nanotube, providing a one-to-one correspondence in property–structure relationship. This is an exciting field in nanoscience and nanotechnology.

ACKNOWLEDGMENTS

The authors are thankful for the financial support of NSF grants DMR-9971412 and DMR-9733160.

The authors also thank the Georgia Tech Electron Microscopy Center for providing the research facility.

REFERENCES

1. Z. L. Wang (ed.), *Characterization of Nanophase Materials*, Wiley-VCH, New York (1999).
2. P. Poncharal, Z. L. Wang, D. Ugarte, W. A. de Heer. *Science* **283**, 1516 (1999).
3. Z. L. Wang, P. Poncharal, W. A. de Heer. *J. Phys. Chem. Solids*, in press (2000).
4. P. Poncharal, S. Frank, Z. L. Wang, and W.A. de Heer, in Proceeding of the International Conference on Small Clusters (Lausanne, 1998).
5. E. Wong, P. Sheehan, C. Lieber. *Science* **277**, 1971 (1997).
6. J. P. Salvetat, A. J. Kulik, J. M. Bonard, G. A. D. Briggs, T. Stockli, K. Metenier, S. Bonnamy, F. Beguin, N. A. Burnham, L. Forro. *Adv. Mater.* **11**, 161 (1999).
7. M. M. Treacy, T. W. Ebbesen, J. M. Gibson. *Nature* **38**, 678 (1996).
8. L. Meirovich. *Element of Vibration Analysis*, McGraw-Hill, New York (1986).
9. W. A. de Heer, A. Chatelain, D. Ugarte. *Science* **268**, 845 (1995).
10. H. J. Dai, E.W. Wong, C. M. Lieber. *Science* **272**, 523 (1996).
11. T. W. Ebbesen, H. J. Lezec, H. Hiura, J. W. Bennett, H. F. Ghaemi, T. Thio. *Nature* **382**, 54 (1996).
12. S. Frank, P. Poncharal, Z. L. Wang W. A. de Heer. *Science* **280**, 1744 (1998).
13. P. J. de Pablo, E. Graugnard, B. Walsh, R. P. Andrews, S. Datta, R. Reifenberger. *Appl. Phys. Lett.* **74**, 323 (1999).